Journal of Fluids and Structures 50 (2014) 340–357

Contents lists available at ScienceDirect

Journal of Fluids and Structures

journal homepage: www.elsevier.com/locate/jfs

Wake-induced vibration of tandem and staggered cylinders with two degrees of freedom

Gustavo R.S. Assi

Department of Naval Architecture & Ocean Engineering, University of São Paulo, NDF, Escola Politécnica, 05508-030 São Paulo, Brazil

ARTICLE INFO

Article history:
Received 3 February 2014
Accepted 2 July 2014
Available online 22 August 2014

Keywords:
Wake-induced vibration
Circular cylinders
Vortex wake
Flow interference

ABSTRACT

The wake-induced vibration (WIV) of two staggered cylinder with two degrees of freedom (2-dof) has been investigated by experiments in a water channel for Reynolds number between 2000 and 25 000. The streamwise separation was fixed to 4 diameters and the lateral separation varied between 0 and 3 diameters for tandem and staggered configurations. Results are presented in the form of trajectories of motion and dynamic response curves of displacements, frequencies and force coefficients. Excitation caused by the WIV mechanism is found to get weaker as the initial position of the downstream cylinder is increased from the centreline of the wake (tandem arrangement) towards the sides. For a lateral separation of 3 diameters wake interference was already found to be negligible. Evidence of a type of wake-stiffness concept is also observed to occur for 2-dof WIV in tandem arrangement, especially for higher reduced velocities. A similar mechanism may also be occurring for staggered arrangements around the centreline.

1. Introduction

The topic of *wake-induced vibration* (WIV) of a pair of interfering cylinders is a fundamental subject in fluid–structure interaction that still draws the attention of many researches. In a few words, WIV is a fluid–elastic mechanism able to excite into oscillatory motion a bluff body immersed in the wake generated from another body positioned upstream. At first sight it appears to be a very simple phenomenon, but careful investigations have uncovered complex mechanisms that can only be understood through the lenses of unsteady fluid–elasticity. In the present study we are concerned with the WIV of the downstream cylinder of a pair arranged in tandem and staggered configurations, i.e. in staggered arrangements the cylinders are not aligned with the flow but offset from the centreline. WIV differs from the well studied phenomenon of *vortex-induced vibration* (VIV)—reviewed by Bearman (1984), Williamson and Govardhan (2004) and others—in the sense that the excitation is not generated in the vortex shedding mechanism of the body itself, but it comes from the interaction of the body with a wake developed further upstream.

It is not difficult to be carried away by the apparent simplicity of the problem and plan or design experiments without considering the number of parameters involved. For example, take two cylinders modelled as rigid bodies with two degrees of freedom (2-dof) each. To start with geometric parameters, there will be two diameters and a streamwise and a cross-flow separation, which will distinguish the tandem from the staggered arrangements. On the structural properties side, there will be different parameters of mass for each cylinder as well as damping and stiffness regarding each direction of motion. After all, a pair of rigid cylinders oscillating in 2-dof will present a dozen of different possible combinations of geometric and

E-mail address: g.assi@usp.br

http://dx.doi.org/10.1016/j.jfluidstructs.2014.07.002
0889-9746/

structural parameters to be considered, not to mention experiments with long flexible cylinders with several modes of vibration. In addition, one may include flow parameters such as speed, velocity profiles and turbulence intensity on the free stream. For this reason, only a few studies that managed to vary one or two parameters at a time were able to contribute to the understanding of the WIV excitation mechanisms and tell it apart from other types of flow-induced vibration of bluff bodies.

Nevertheless, WIV has been revisited by quite a few papers in the recent years. In addition to the papers pointed out along this text, one should refer to the book of Paidoussis et al. (2011) and the comprehensive review paper published by Sumner (2010) as a means to finding old and new literature on the topic of wake interaction. WIV has also been referred to by different names in the past literature, such as 'wake-induced galloping' (Bokaian and Geoola, 1984) and 'wake-displacement excitation' (Zdravkovich, 1988). But we shall follow Assi et al. (2010) and keep the terminology *wake-induced vibration* not to mistake it by 1-dof vibrations normally associated with classical galloping of non-axisymmetric cross-sections.

Bokaian and Geoola (1984) and Assi et al. (2010, 2013) have studied the flow-induced vibration of the downstream cylinder moving only in the cross-flow direction in water channels. Simpson (1977), on the other hand, has investigated the streamwise instabilities of a pair of tandem cylinders in a wind tunnel. Several models have been developed to capture the mechanisms behind this type of flow-induced vibration, most of them starting from quasi-steady assumptions but adding time delays to account for the unsteady effects of the wake–structure interaction (a review of these models is found in Price, 1995). Simpson and Flower (1977) enhanced the quasi-steady model including movements of the upstream cylinder. Tsui and Tsui (1980) further developed an instability analysis for when the cylinders are mechanically coupled. And the nonlinear analysis performed by Price and Abdallah (1990) revealed interesting results about the effect of damping and frequency detuning on the response. Most of these works have been concerned with the vibration of the downstream cylinder undergoing a type of mechanism called 'wake flutter', in which the cylinder is able to extract energy from the flow as it oscillates in an elliptical orbit within the upstream wake. Price (1975), Price and Abdallah (1990) and Naudascher and Rockwell (1994) offer clear descriptions with illustrated explanations of this mechanism.

Fig. 1 presents the velocity field obtained with PIV (particle-image velocimetry) around two static cylinders in staggered arrangements. PIV was performed at mid length to characterise steady wake topology; details on the set-up are presented in Assi (2009). As the downstream cylinder moves away from the centreline, the wake interference from the upstream cylinder is reduced. For the tandem arrangement, in Fig. 1(a), the upstream wake is symmetrically split around the downstream body, while for the staggered configurations in (b) and (c) the upstream wake interferes with the inner side of the second cylinder. Streamlines show that the steady wake of the upstream cylinder is displaced by the presence of the second body. For a lateral separation of $y_0/D = 3.0$ the downstream cylinder appears to be so far out of the upstream wake that its wake symmetry is almost recovered.

We believe Fig. 1 illustrates rather well the phenomenon described by Zdravkovich (2003) as '*wake-displacement*' when he writes that "the downstream cylinder is not *immersed* in the upstream cylinder wake but *displaces* it instead". However, as shown by Assi et al. (2013), the unsteady flow field around a static downstream cylinder is quite different from that around a cylinder that is not moving across the wake. In fact, the unsteady wake interference was found to be fundamental to excite WIV. Assi et al. (2010) showed how the instantaneous vortex interference may enhance or diminish lift depending on the wake pattern. Hence the time-averaged flow fields in Fig. 1 are very limited in terms of information they provide for an investigation of the unsteady phenomenon. Nevertheless, they show how far out of the centreline the downstream cylinder needs to be in order for wake interference to become insignificant, setting the boundaries for the present study.

2. Method

The present paper is a follow-up on the previous works of Assi et al. (2010, 2013) so, in order to avoid unnecessary lengthy repetition, the reader will be constantly referred to those papers. In those previous works we kept constant as many parameters as possible in order to investigate the intricate mechanisms of wake interference. Only allowing for the downstream cylinder of a tandem pair to respond to flow excitation in the cross-flow direction made it possible to identify the complex unsteady excitation mechanism by vortex–structure interaction and the powerful concept of wake stiffness. Now, in the present study, we shall release some constraints adding new parameters to the investigation.

The basic arrangement is illustrated in Fig. 2. The initial position of the downstream cylinder can be varied from the tandem arrangement (in which both cylinders are aligned with the flow direction) to staggered configurations changing the lateral spacing between the bodies, hence x_0 and y_0 define the initial geometry of the pair. The streamwise separation, measured from centre to centre, was kept fixed at $x_0/D = 4.0$ at all times and y_0/D was varied between 0 and 3. The upstream cylinder was always static while the downstream cylinder was allowed to respond with oscillations in 2-dof in the cross-flow (y) and streamwise (x) directions. Although this represents only a sample of the multi-parametric universe, by testing the system on these conditions we may identify some general characteristic behaviours. For example, we will be able to notice the decreasing effect of the WIV mechanism as the downstream cylinder moves away from the centreline of the wake and we will see evidence for the existence of 'wake-stiffness' for configurations other than the tandem arrangement (to be described later).

Fig. 3, reproduced from Assi et al. (2010), presents the WIV response of the downstream cylinder of a tandem pair free to respond in one degree of freedom (1-dof) in the cross-flow direction. The top graph shows the variation of the amplitude of

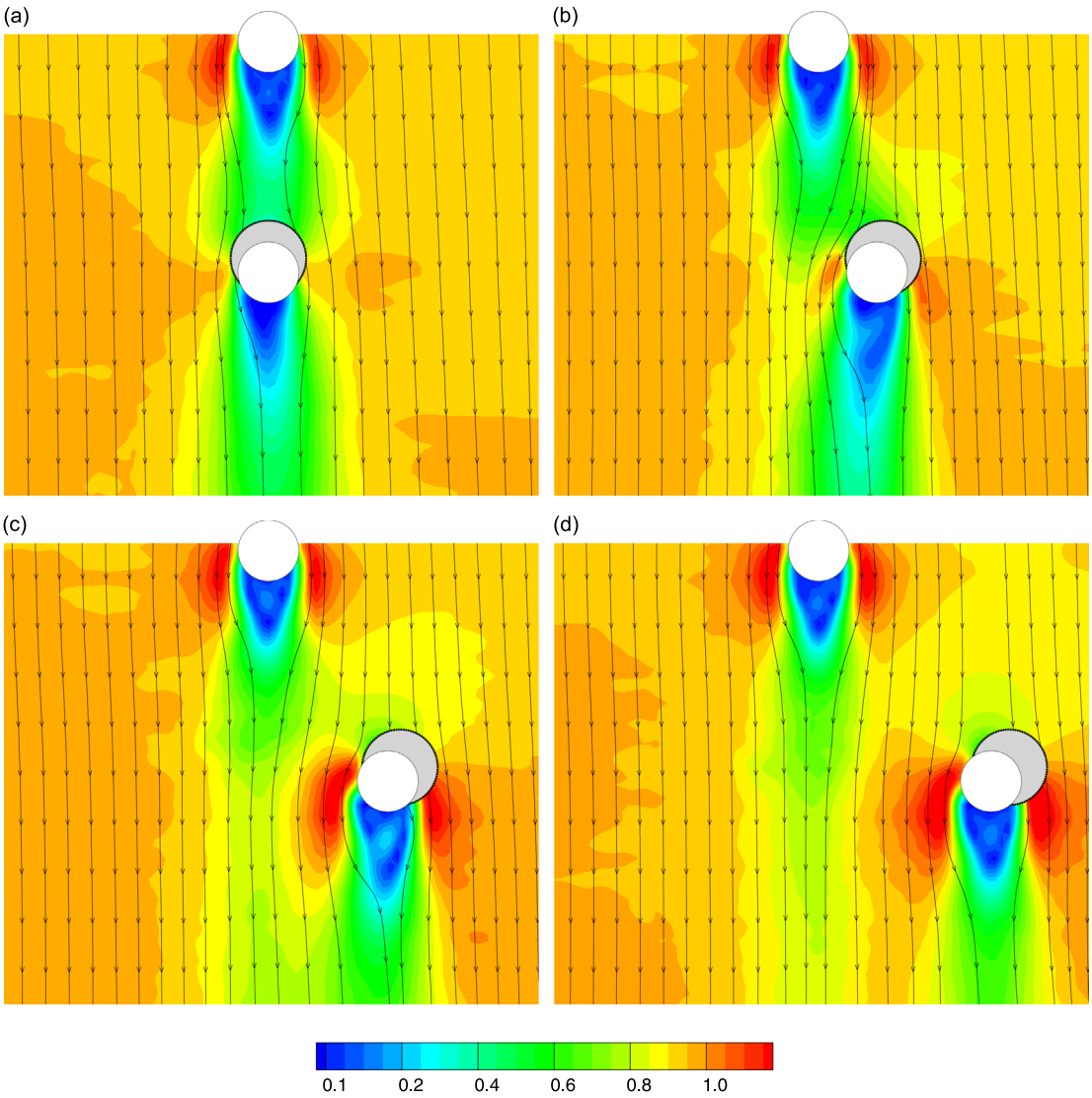

Fig. 1. Steady flow velocity field around a pair of static cylinders. Contours of velocity magnitude normalised by free stream velocity. Re = 19 200, $x_0/D = 4.0$ and (a) $y_0/D = 0.0$, (b) $y_0/D = 1.0$, (c) $y_0/D = 2.0$, (d) $y_0/D = 3.0$.

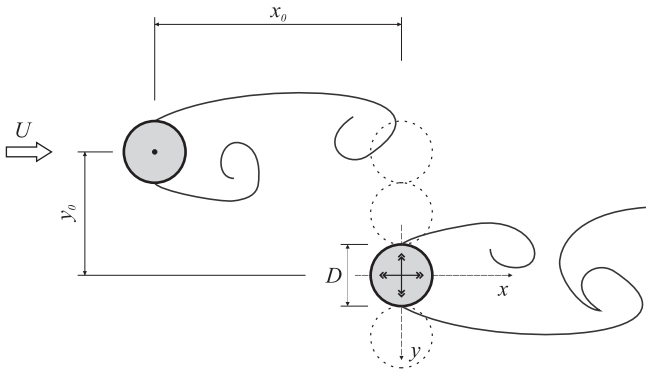

Fig. 2. Arrangement for a pair of tandem and staggered cylinders. The initial streamwise spacing was fixed at $x_0/D = 4.0$ and the lateral spacing varied between $y_0/D = 0.0$, 1.0, 2.0 and 3.0. Solid lines represent hypothetical interaction between the shear layers.

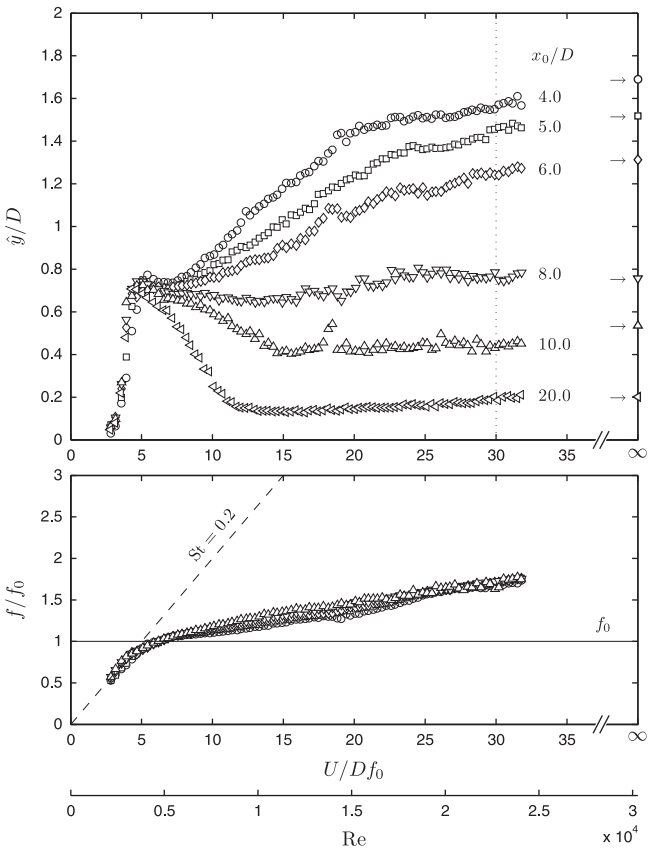

Fig. 3. WIV response of the downstream cylinder with 1-dof for various x_0/D separations. *(top)* Displacement and *(bottom)* dominant frequency of oscillation. Reproduced from Assi et al. (2010).

vibration for various tandem separations (x_0/D) between 4 and 20 diameters. One immediately notices that the interference effect from the upstream wake reduces as the second cylinder is moved further downstream. But it is interesting to note that even for a large gap of $x_0/D = 10$ the vibration of the downstream cylinder still is influenced by the upstream wake. It was only for $x_0/D = 20$ that the typical VIV response of an isolated cylinder was recovered.

Another interesting aspect of WIV lies in the frequency signature of the response. In the bottom graph of Fig. 3 it becomes evident that, independently of the separation, the downstream cylinder presents a rather well behaved and predictable frequency of vibration. Assi et al. (2013) later pointed out that this response frequency is a signature of the WIV mechanism and could be associated with the concept of wake stiffness, which dominates over the structural stiffness for higher reduced velocities. They argued that the wake–structure interaction creates a restoring force of hydrodynamic nature that confers the system a kind of characteristic frequency of vibration.

Now, if the initial position of the cylinders is altered to staggered configurations it is expected that the WIV response will also change, since the downstream cylinder will oscillate in regions of different wake interferences. Zdravkovich (1988) mapped the wake downstream of the first static cylinder regarding the wake interference on the second static body and Sumner et al. (2000) investigated the flow patterns of the wake around several staggered configurations. Fig. 4 identifies a region of 'proximity interference' for various staggered arrangements when the streamwise separation is less than a critical value around $x_0/D = 3.5$. Flow-induced vibration in this region is driven by different mechanisms other than WIV and will not be covered in the present study. For an investigation of 'interference galloping' of the cylinder at close proximity the reader should refer to Ruscheweyh (1983), who performed tests with an elastic cylinder in a wind tunnel to explain the excitation from hysteretic flow-switching in the gap between the cylinders (later verified in waterchannel experiments by Ruscheweyh and Dielen, 1992). A second region identified as 'wake interference' appears for tandem and staggered configurations up to $y_0/D \approx 1.5$ independently of streamwise separation. In this region the WIV mechanism described in Assi et al. (2010, 2013) takes place. Finally, another region identified as 'no interference' appears when the downstream cylinder is located out of the reach of the upstream wake for $y_0/D > 1.5$.

In the present study we shall focus on the response of the downstream cylinder in 2-dof at $x_0/D = 4.0$ in order to avoid close 'proximity interference' and a response excited by 'interference galloping'. Four lateral separations will vary between $y_0/D = 0$ and 3. According to the static map of Zdravkovich (1988) the cylinder should move from the strongest 'wake

interference' region out of the upstream wake to the 'no interference' region without passing through the 'proximity interference' region.

3. Experimental setup

Experiments were performed in the Department of Aeronautics at Imperial College, London, in a recirculating water channel with a test section 0.6 m wide, 0.7 m deep and 8.4 m long. Flow speed, U, could be continuously varied up to 0.6 m/s with free stream turbulence intensity around 3%. The actual flow quality was proved to be adequate to perform flow-induced vibration tests and preliminary results were validated in Assi et al. (2010) against other experiments presented in the literature. A pair of cylinders was arranged in the test section, as illustrated in Fig. 2, at $x_0/D = 4.0$ and $y_0/D = 0.0$, 1.0, 2.0 and 3.0. Measurements of displacement were taken in relation to the initial position of the downstream cylinder, i.e. the origin of the x and y axes in Fig. 2.

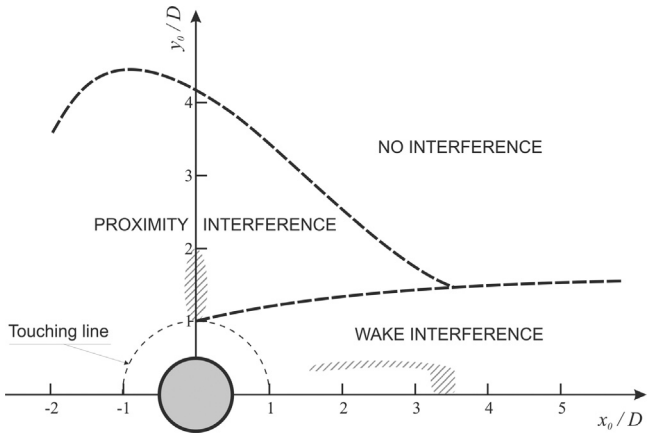

Fig. 4. Sketch of interference regions for static cylinders. Hatched areas mean bistable flow regions. Adapted from Zdravkovich (1988).

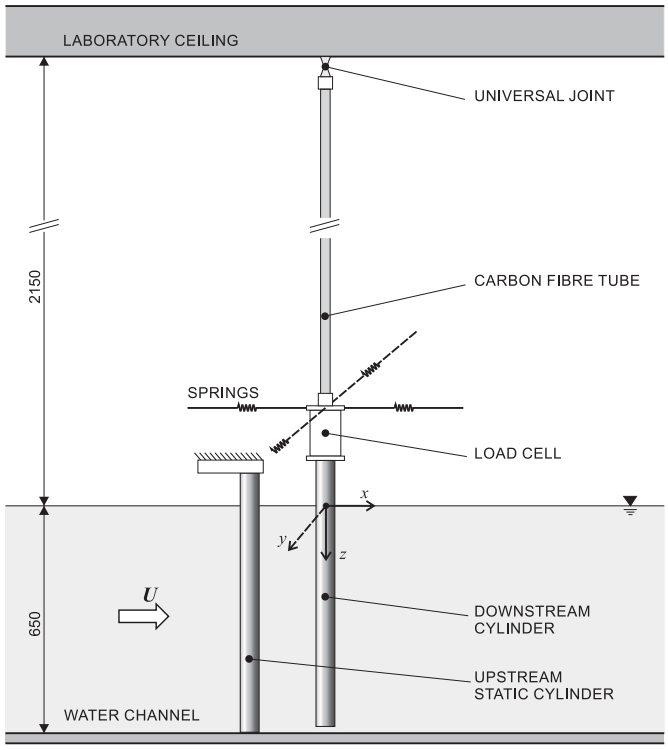

Fig. 5. Schematic representation of the experimental setup with the 2-dof pendulum rig holding the downstream cylinder. (Units are in millimetres.)

A schematic representation of the experimental setup is shown in Fig. 5. Circular cylinder models were made from a 50 mm-diameter acrylic tube, giving a maximum Reynolds number of approximately 30 000, based on cylinder diameter, D, at $U=0.6$ m/s. With a wet-length of 650 mm, the resulting aspect ratio of the model was 13. The upstream cylinder was rigidly attached to the structure of the channel preventing displacements in any direction, while the downstream cylinder was fixed from its upper end to a 2-dof elastic rig that allowed the cylinder to freely respond in both cross-flow and streamwise directions. The downstream cylinder was mounted at the lower end of a long carbon-fibre tube which formed the arm of a rigid pendulum and was connected to a universal joint fixed at the ceiling of the laboratory.

A small gap of 2 mm was left between the bottom of the downstream cylinder and the floor of the test section. Although end conditions were different at the extremities of the cylinder, flow visualisations showed that vortex shedding remained

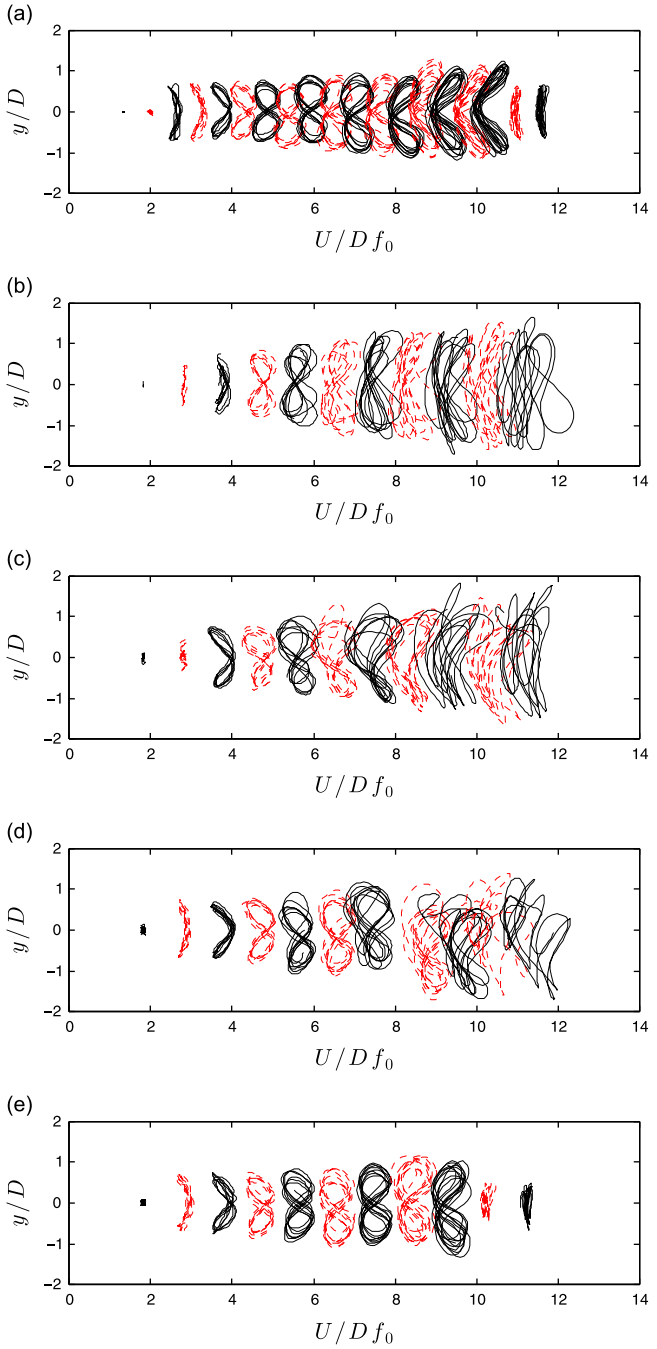

Fig. 6. Trajectories of motion versus reduced velocity for (a) a single cylinder and the downstream cylinder of a pair at $x_0/D=4.0$, (b) $y_0/D=0.0$, (c) $y_0/D=1.0$, (d) $y_0/D=2.0$, (e) $y_0/D=3.0$.

parallel to the cylinder for all flow speeds. The distance between the bottom of the cylinder and the pivoting point of the universal joint was 2800 mm, hence for a displacement equal to 1 diameter the inclination angle of the cylinder was only just over 1 degree from the vertical. Two independent optical sensors were employed to measure displacements in the *x* and *y*-directions; all displacement amplitudes presented for 2-dof measurements are for a location at the mid-length of the model.

Two pairs of coil springs were installed in the *x* and *y*-axes allowing the setting of different natural frequencies in the cross-flow and streamwise directions, f_{0_y} and f_{0_x}, respectively. Although the cylinder was initially aligned in the vertical position, in flowing water the mean drag displaced the cylinder from its original location. To counteract this effect the in-line pair of springs was attached to a frame that could be moved back and forth in the direction of the flow. For each flow speed there was a position of the frame that maintained the mean position of the cylinder within 10% of a diameter from the original vertical arrangement, balancing the drag force with the displacement of the springs. This was more difficult to achieve for higher reduced velocities due to the unsteady nature of the phenomenon, as will be explained later. It was a compromise in either altering the mean position or allowing the cylinder to freely respond. In the end it was preferable to

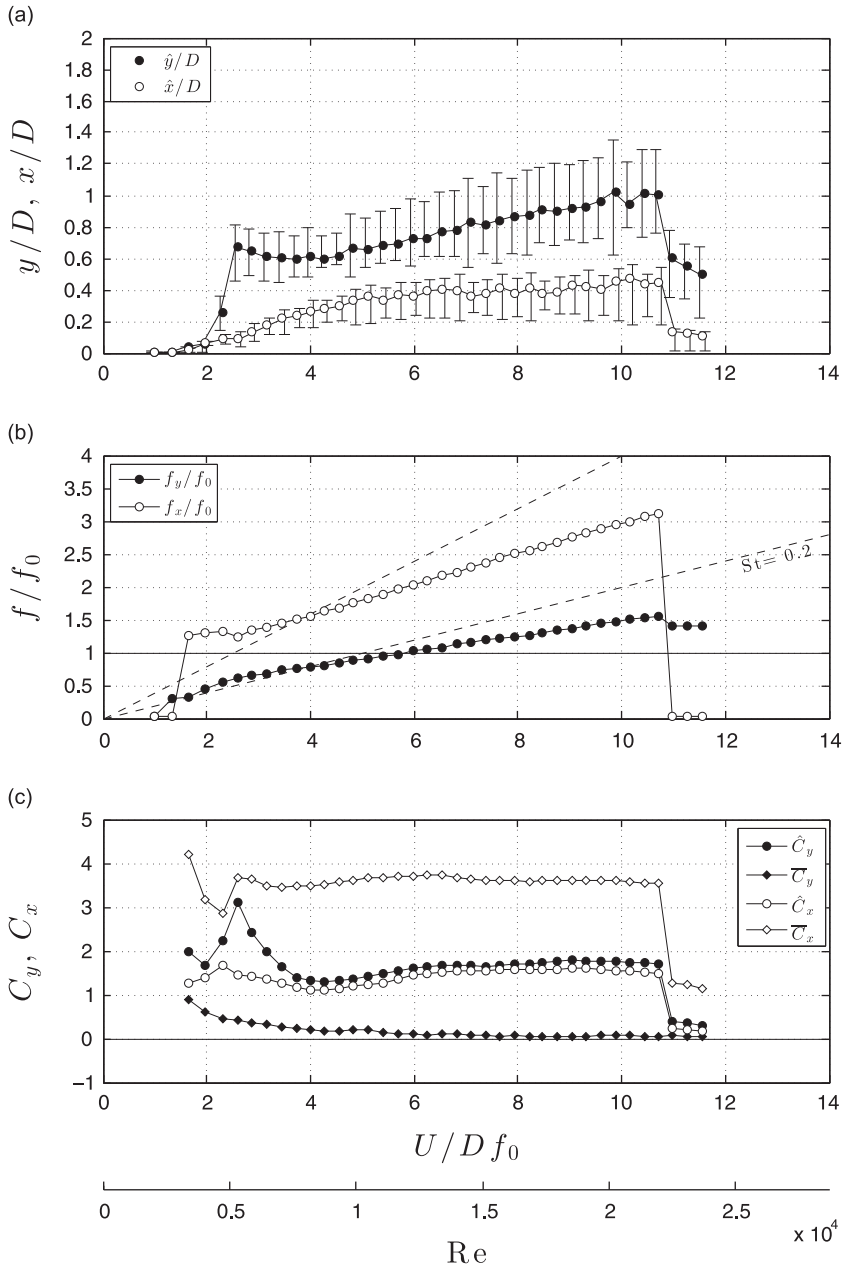

Fig. 7. VIV dynamics response of an isolated cylinder. (a) Displacement and (b) frequency of vibration and (c) force coefficients.

keep the parameter x_0 constant, thus favouring parametric analyses. Using two pairs of springs perpendicular to each other resulted in nonlinear spring constants for large displacements in the transverse and in-line directions. Movement in the transverse direction will cause a lateral spring deflection in the in-line direction and vice versa. This nonlinearity was minimised by making the springs as long as possible, hence the in-line springs were installed at the end of 4 m-long wires fixed at the extremities of the frame.

It is known that during the cycle of vortex shedding from bluff bodies the fluctuation of drag has double the frequency of the fluctuation of lift. Hence a particularly severe vibration might be expected to occur if the hydrodynamic forces in both directions could be in resonance with both in-line and transverse natural frequencies at the same time. For this reason, we set f_{0_x} to be close to twice of f_{0_y} by adjusting the stiffness of both pairs of springs. Values for f_{0_x}, f_{0_y} and ζ were determined by measuring free oscillations in air in both directions. In fact, the actual value turned out to be $f_{0_x}/f_{0_y} = 1.9$. In the reduced velocity parameter, U/Df_0, the frequency f_0 is the natural frequency in the cross-flow direction f_{0_y}. The mass ratio was found to be $m^* = 1.6$, defined as the ratio between the total oscillating mass to the mass of displaced fluid. The structural damping $\zeta = 0.3\%$, represented as a fraction of the critical damping, was practically the same for both directions of motion.

A load cell was attached at each cylinder to measure instantaneous and time-averaged hydrodynamic forces—inertial components have been subtracted from the total force acquired by the load cell, find details in Assi et al. (2009). Total lift was divided into mean ($\overline{C}_y$) and r.m.s. ($\hat{C}_y$) components. The same applied to the drag coefficient ($\overline{C}_x$ and $\hat{C}_x$). Each data point presented in the following section is composed of more than 200 cycles of vibration on that specific reduced velocity.

4. Results and discussion

Results are presented in the form of trajectories of motion and curves of the dynamic response of displacement and frequency. Hydrodynamic force coefficients are also presented for all configurations compared with those for an isolated cylinder.

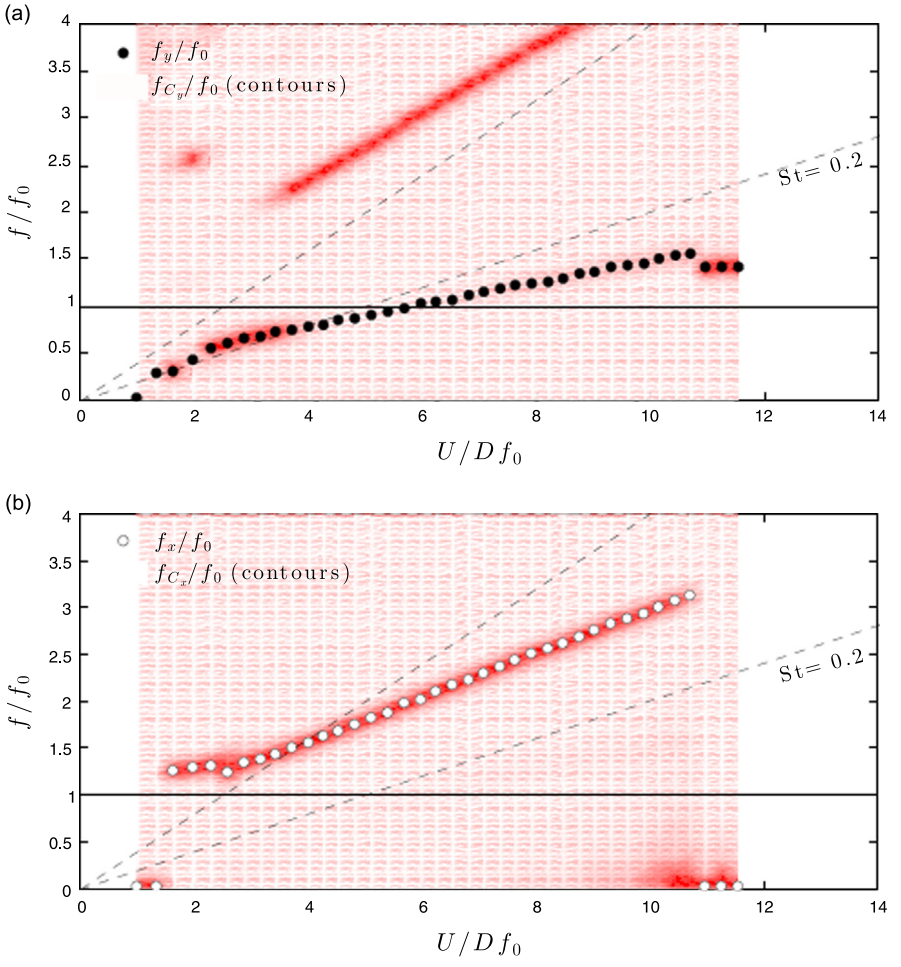

Fig. 8. Dominant frequency of vibration (symbols) and power spectrum (background red contours) of (a) lift and (b) drag for an isolated cylinder. (For interpretation of the references to colour in this figure caption, the reader is referred to the web version of this paper.)

4.1. Trajectories of motion

Before going into the details of the response for all staggered configurations we shall start by an overall qualitative comparison between the response of an isolated cylinder under VIV and the tandem and staggered cases under WIV. Fig. 6 compares 2-dof trajectories of motion versus reduced velocity for all investigated cases. The x-axis for displacement is not shown in the figure for clarity, but it has the same scale as the y-axis. Also, trajectories alternate in colour and line style for clarity.

Fig. 6(a) presents the typical trajectories of motion for a single cylinder under 2-dof VIV in which the f_{0_x} is almost twice as f_{0_y}. As reduced velocity is increased vibrations start to build up in a 'C' shape, changing into '8'-shaped curves until the end of the synchronisation range at around reduced velocity 12. The overall response was found to be in good agreement with results found for $f_{0_x}/f_{0_y} = 1.9$ in Fig. 4 of Dahl et al. (2006) and those of Assi et al. (2009).

The 2-dof response of the downstream cylinder of a tandem pair is presented in Fig. 6(b). As expected, trajectories are very different from those of the typical VIV response of an isolated cylinder due to the interference effect of the upstream wake. It is evident that both streamwise and cross-flow displacements are increased when compared to Fig. 6(a), but one may also note that the cycles of WIV are not as repeatable as those for VIV, especially for reduced velocities above 6 when the WIV mechanism dominates over VIV. One may argue about the non-existence of harmonic motion in WIV, but the fact is that each cycle of vibration will be the result of interference with different wake patterns (as proposed by Assi et al., 2010), resulting in a unique trajectory at each cycle but with overall periodic characteristics.

In Fig. 6(c) we find the response of a staggered cylinder initially dislocated from the centreline of the upstream wake by 1D. The trajectories manage to capture the asymmetry in the wake interference by showing one loop of the '8' shapes larger than the other. For reduced velocities above 9 the '8'-shaped cycles tend to disappear and the trajectories take the form of periodic orbits that could be associated with 'wake flutter' (to be discussed later).

The wake interference effect is further reduced as the cylinder moves out of the upstream wake, as observed in Fig. 6(d) for a staggered configuration of $y_0/D = 2.0$. The asymmetry in motion is still perceived, but rather weakened when compared to Fig. 6(c). For the last staggered arrangement of $y_0/D = 3.0$, presented in Fig. 6(e), the downstream cylinder finds itself too far out of the upstream wake that almost no interference is observed in the response. The trajectories resemble that of an isolated cylinder in VIV, not quite like those observed in Fig. 6(a), but still very different from Fig. 6(b)–(d).

According to Zdravkovich (1988), somewhere between $y_0/D = 1.0$ and 2.0 a static downstream cylinder should cross the boundary from the 'wake interference' to the 'no interference' region (Fig. 4). However, when the downstream cylinder is oscillating with high amplitudes of motion it is expected that wake interference will occur for initial separations further out of the centreline, since the cylinder moves in and out of the 'wake interference' zone. This is made clear by the fact that a significant change in the response seen in Fig. 6(d) and (e) was only achieved when the downstream cylinder was moved from $y_0/D = 2.0$ to 3.0.

4.2. Displacement, frequency and force coefficients

Moving on to a more detailed analysis involving displacements, frequencies and hydrodynamic forces we come to Fig. 7, which will serve as a reference presenting the response of an isolated cylinder in 2-dof VIV.

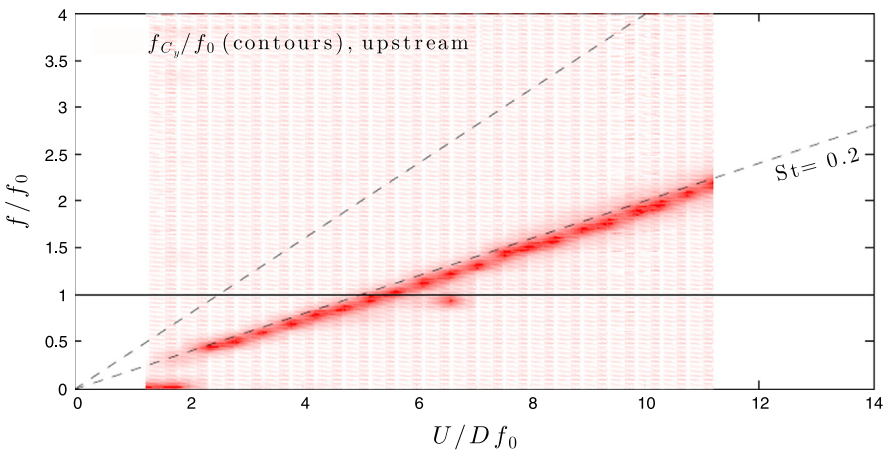

Fig. 9. Power spectrum (red contours) of lift for the upstream cylinder of a tandem pair. Identical plots were obtained for all staggered arrangements. (For interpretation of the references to colour in this figure caption, the reader is referred to the web version of this paper.)

4.2.1. Isolated cylinder

Fig. 7(a) presents the amplitudes of displacement in the cross-flow ($\hat{y}/D$) and streamwise ($\hat{x}/D$) directions nondimensionalised by the cylinder diameter. The amplitudes $\hat{y}$ and $\hat{x}$ represent the so called harmonic amplitude of motion, calculated as the r.m.s. of the signal multiplied by $\sqrt{2}$. Vertical bars associated with each data point represent an estimation of the maximum and minimum peaks of vibration achieved for each reduced velocity. In fact, the bars have been calculated taking an average of the 25% highest and lowest peaks for each time series constituted of more than 200 cycles of oscillation. Therefore, for a given reduced velocity it is possible to evaluate the average amplitude of vibration as well as variations in the envelope of vibration through time. Larger bars mean that the displacement presents considerable variation from cycle to cycle.

In Fig. 7(a) the synchronisation range of VIV is clearly identified by a rise in amplitude in both $\hat{y}/D$ and $\hat{x}/D$ roughly between reduced velocities 2 and 11. A maximum amplitude of $\hat{y}/D \approx 1.0$ is achieved at the end of the synchronisation

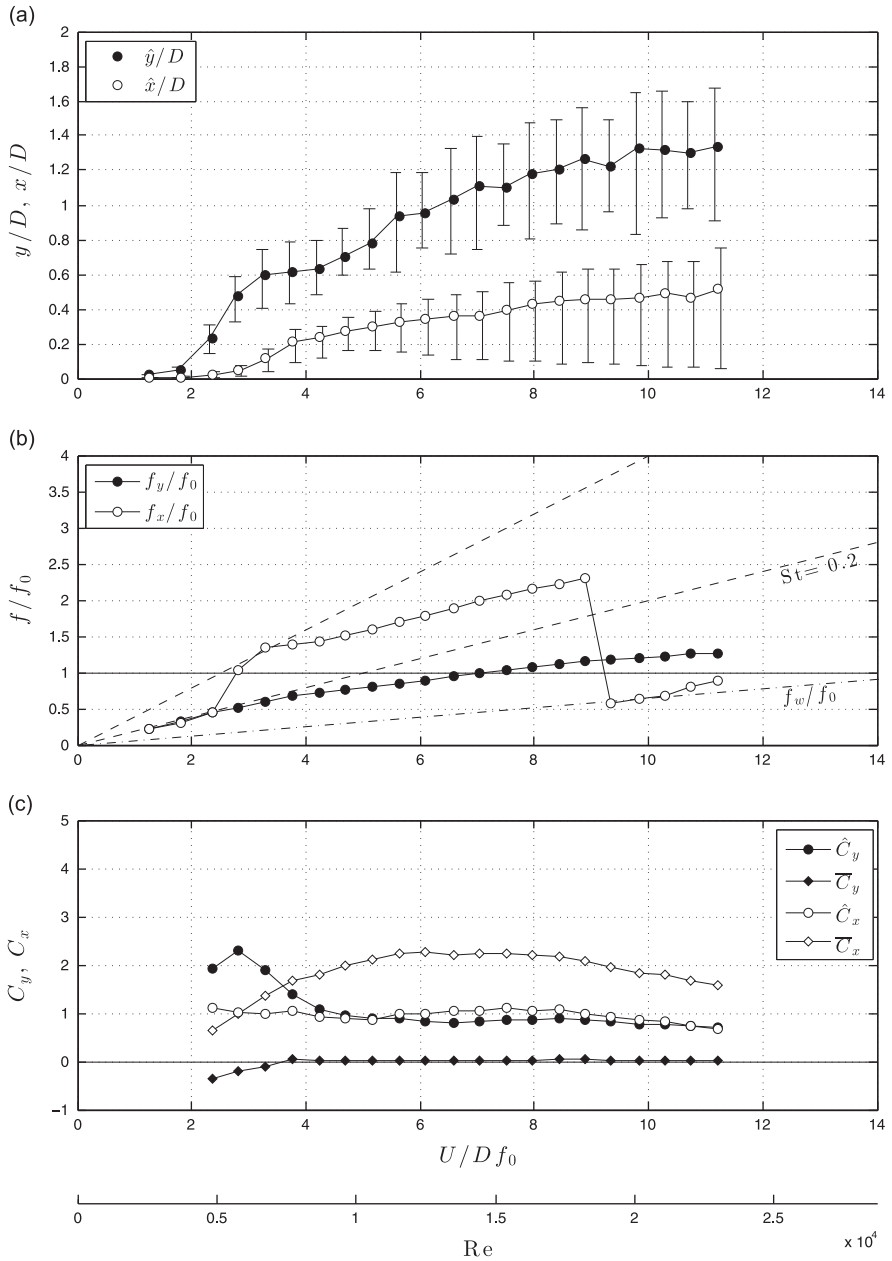

Fig. 10. WIV dynamic response of the downstream cylinder in tandem arrangement, $x_0/D = 4.0$ and $y_0/D = 0.0$. (a) Displacement and (b) frequency of vibration and (c) force coefficients.

range, just before a sudden drop in response in both directions. This is typical of the 2-dof VIV response of a single cylinder with $f_{0_x}/f_{0_y} \approx 2$ and has been reported by Dahl et al. (2006) and Assi et al. (2009), among others.

The dominant frequencies of vibration nondimensionalised by f_0 are plotted in Fig. 7(b). Both f_y/f_0 and f_x/f_0 follow clear trends in which the streamwise vibration shows double the frequency of the cross-flow direction, as expected. Two dashed lines mark the equivalent frequency for a hypothetical Strouhal number of 0.2 and twice as that. Fig. 8 presents the same frequency data in a slightly different manner. The same dominant frequency data points are plotted over the normalised power spectrum of the hydrodynamics force associated to each direction. Darker areas represent peaks in the spectrum. So, in Fig. 8(a) it becomes clear that although the preferred frequency of oscillation follows very closely the St=0.2 line, the lift force measured on the cylinder presents clear evidence of the third harmonic. In Fig. 8(b) only one single branch is identified in the spectral signature of drag, which obviously corresponds to the dominant f_x/f_0. For details about how the spectrum plots were created refer to Assi (2009).

Returning to Fig. 7(c), the mean and fluctuating components of lift and drag are presented for almost the whole range of reduced velocities. A few data points for the lowest reduced velocities have been excluded due to the high experimental uncertainty in measuring minute hydrodynamic forces caused by very low flow speeds; data points for $U/Df_0 < 2$ were kept in the figures but must be considered with caution since uncertainties are still high. Nevertheless, the typical amplification of $\overline{C}_x$ and $\hat{C}_y$ is observed to occur during the synchronisation range. It is difficult to find similar measurements in the literature, but our results show some agreement with those of Jauvtis and Williamson (2004), at least as far as orders of magnitude are concerned.

4.2.2. *Tandem arrangement*

The spectrum of lift on the upstream static cylinder has also been measured in a similar way, as presented in Fig. 9 for when the cylinders are arranged in tandem ($y_0/D = 0.0$). It reveals that the upstream cylinder is shedding vortices as an

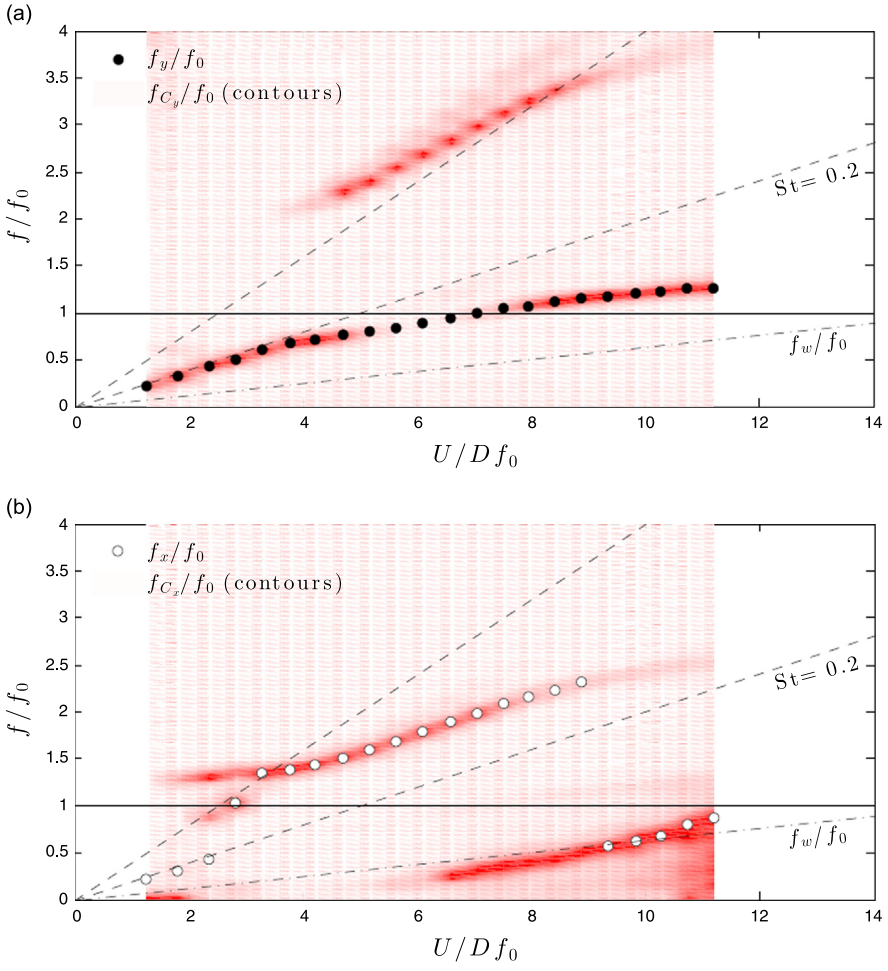

Fig. 11. Dominant frequency of vibration (symbols) and power spectrum (background red contours) of (a) lift and (b) drag for the downstream cylinder of a tandem pair: $x_0/D = 4.0$ and $y_0/D = 0.0$. (For interpretation of the references to colour in this figure caption, the reader is referred to the web version of this paper.)

isolated cylinder, with the frequency of lift clearly following the St=0.2 line. Identical plots were obtained for the upstream cylinder for all tandem and staggered configurations, thus not repeated here for brevity. We conclude that the upstream cylinder (or its vortex shedding mechanism, to be precise) is not affected by the presence or movement of the downstream cylinder in any of the four tested arrangements if $x_0/D \geq 4.0$.

Fig. 10(a) presents the WIV response for the downstream cylinder in tandem arrangement ($y_0/D = 0.0$). As seen in the trajectories of motion in Fig. 6, the displacements are very different from the VIV of a single cylinder due to wake interference. Similar to what was observed for 1-dof WIV of tandem cylinders (Assi et al., 2010), there is no synchronisation range in the WIV excitation, but both $\hat{y}/D$ and $\hat{x}/D$ increase in amplitude with increasing reduced velocity. The variation between maximum and minimum peaks also increases for both cross-flow and streamwise vibrations.

The dominant frequency plot in Fig. 10(b) shows an interesting result. Once more f_y/f_0 and f_x/f_0 seem to follow clear lines that are multiples of each other for most of the reduced velocity range. However, close to the end of the experiments at around $U/Df_0 = 9.0$, the dominant f_x/f_0 jumps to a much lower frequency branch and remains there until the end of the

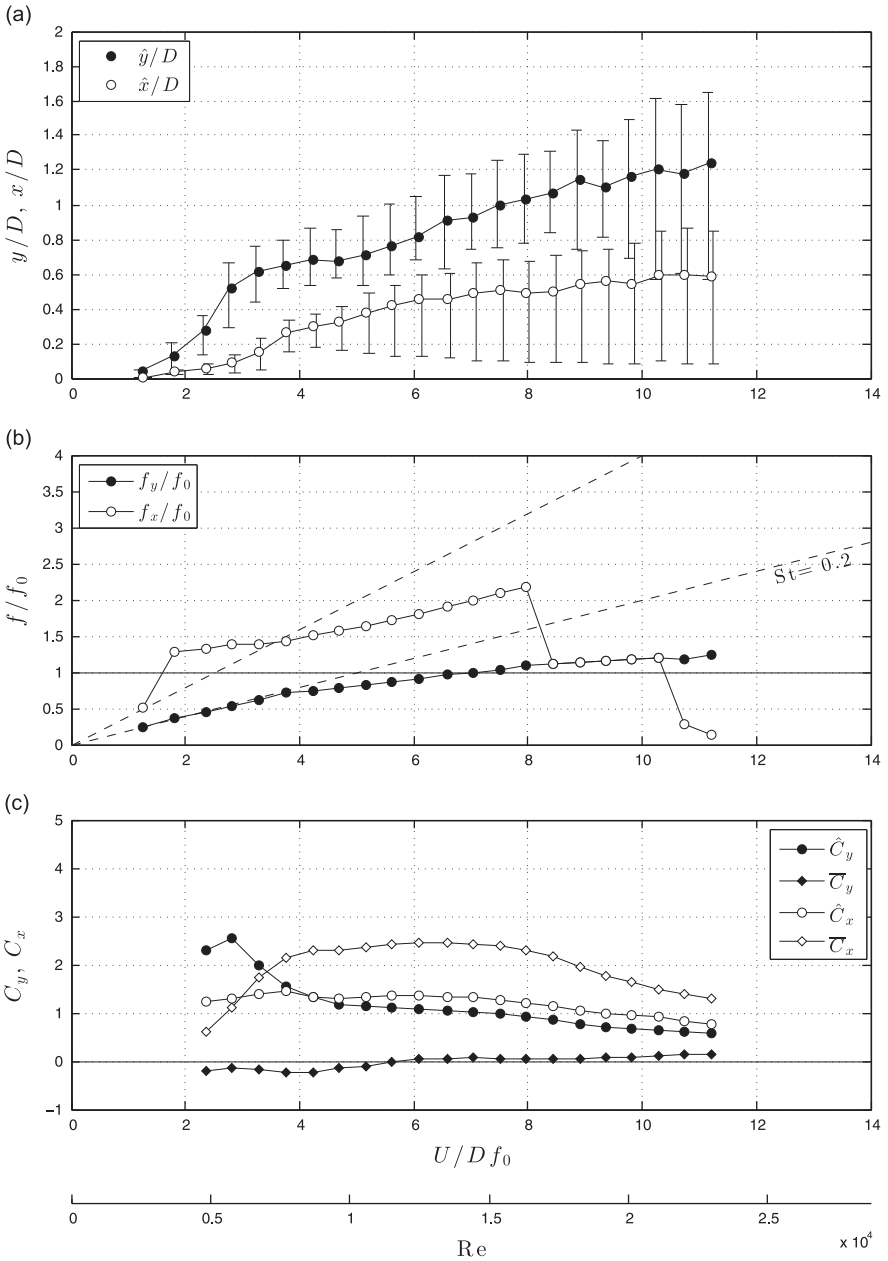

Fig. 12. WIV dynamic response of the downstream cylinder in staggered arrangement, $x_0/D = 4.0$ and $y_0/D = 1.0$. (a) Displacement and (b) frequency of vibration and (c) force coefficients.

reduced velocity range. Looking at the power spectrum of lift and drag in Fig. 11, we verify two branches in Fig. 11(a) for the lift signature (the highest corresponding to the third harmonic), and two branches in Fig. 11(b) for drag. Now, the lowest branch in the drag signature is the one that dominates the frequency of response for reduced velocities above 9. If we take the concept of wake stiffness developed by Assi et al. (2013) for tandem cylinders at $x_0/D = 4.0$ and plot the corresponding wake-stiffness frequency as a dash-dotted line f_w/f_0 in the frequency plots we find that the lowest branch observed in the drag spectrum is indeed very close to f_w/f_0. The same dash-dotted line was added to Fig. 10(b).

We know that for higher reduced velocities around 9 or 10 the resonant effect of VIV is getting weaker as we approach the end of the synchronisation range (Assi et al., 2013). So, for higher reduced velocities the response is totally governed by WIV, hence the wake stiffness could be playing some role in the response, even though the system now has 2-dof. If it is not a coincidence that the dominant f_x/f_0 is so close to f_w/f_0—it might as well be the case—we are left with an open question: why do traces of 'wake-stiffness' frequency appear for vibrations in the streamwise direction rather than in the cross-flow direction? Further investigation, perhaps restraining the cross-flow degree of freedom, may be required for an answer.

The hydrodynamic coefficients in Fig. 10(c) show the amplification of $\overline{C}_x$ due to vibration but with a reduction caused by the shading effect of the upstream wake, as expected. $\overline{C}_y$ is very close to zero (within the experimental uncertainty for force measurements) as a result of a symmetric wake interference.

4.2.3. Staggered arrangements

Fig. 12 presents the WIV response for the downstream cylinder in staggered arrangement with $y_0/D = 1.0$. The overall displacements in Fig. 12(a) are not very different from the tandem configuration, showing that the downstream cylinder is still under a similar interference effect of the upstream wake. The top amplitude of $\hat{y}/D \approx 1.2$ obtained for the highest

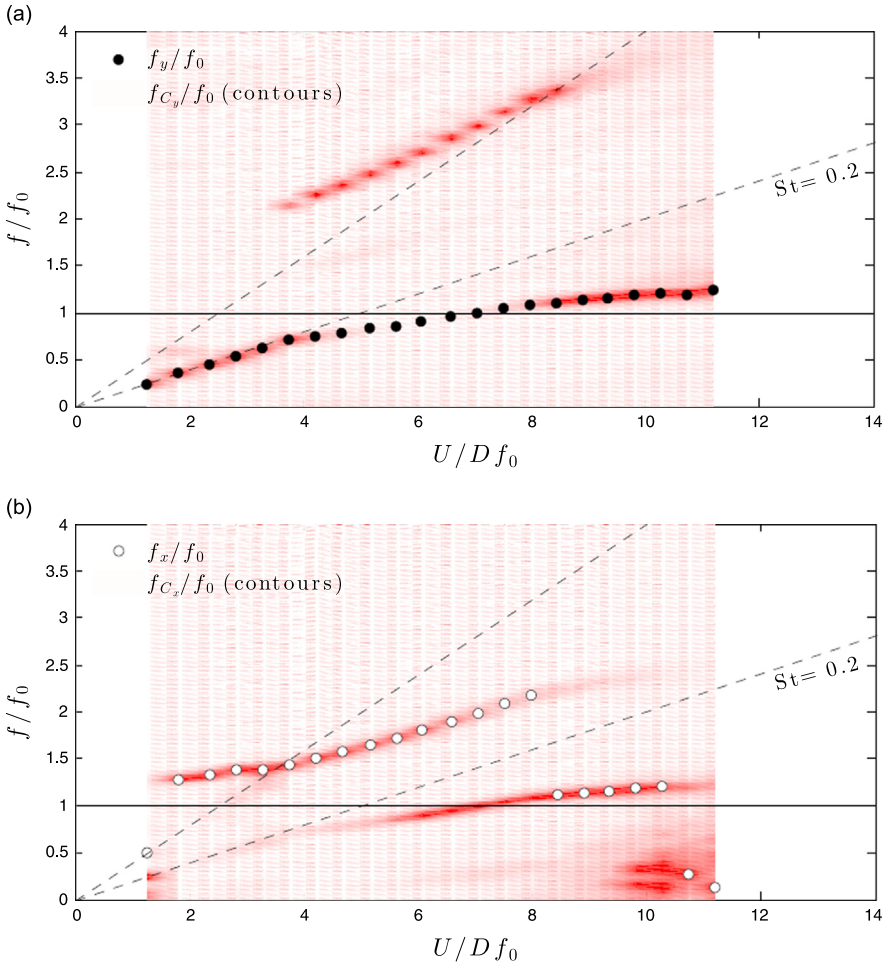

Fig. 13. Dominant frequency of vibration (symbols) and power spectrum (background red contours) of (a) lift and (b) drag for the downstream cylinder of a tandem pair: $x_0/D = 4.0$ and $y_0/D = 1.0$. (For interpretation of the references to colour in this figure caption, the reader is referred to the web version of this paper.)

reduced velocity is slightly reduced when compared to the tandem case. On the other hand, the maximum $\hat{x}/D$ is increased to 0.6. The vertical bars indicate that the envelope of vibration shows an even greater peak variation between cycles.

Again, the frequency curves in Fig. 12(b) bring the most interesting results. Up to reduced velocity 8 both f_y/f_0 and f_x/f_0 are very similar to the tandem case. But for higher reduced velocities the cylinder vibrates with the same frequency in both directions, at least up to $U/Df_0 \approx 10.5$. This congruence of frequencies results in the kind of orbit trajectories seen in Fig. 6(c). In fact, the response for high reduced velocities at this $y_0/D = 1.0$ separation might be governed by 'wake flutter' on top of WIV. Theoretically, 'wake flutter' can be excited in spite of the unsteadiness of the flow, being sustained only by the steady fluid forces present in the wake. Force maps presented in Price (1975) and Assi et al. (2010) show that a static downstream cylinder will be subjected to changes in the steady fluid forces for considerably large separations. A reduced drag force has minimum values on the centreline of the wake and a steady lift force develops maximum values close to the wake interference boundary around $y_0/D = 1.0$. If the downstream cylinder is able to respond in two degrees of freedom (as is the case here) following an elliptical orbit it will move across different gradients of steady lift and drag. A counter-clockwise orbit on the starboard side of the wake extracts energy from the flow to sustain the oscillations.

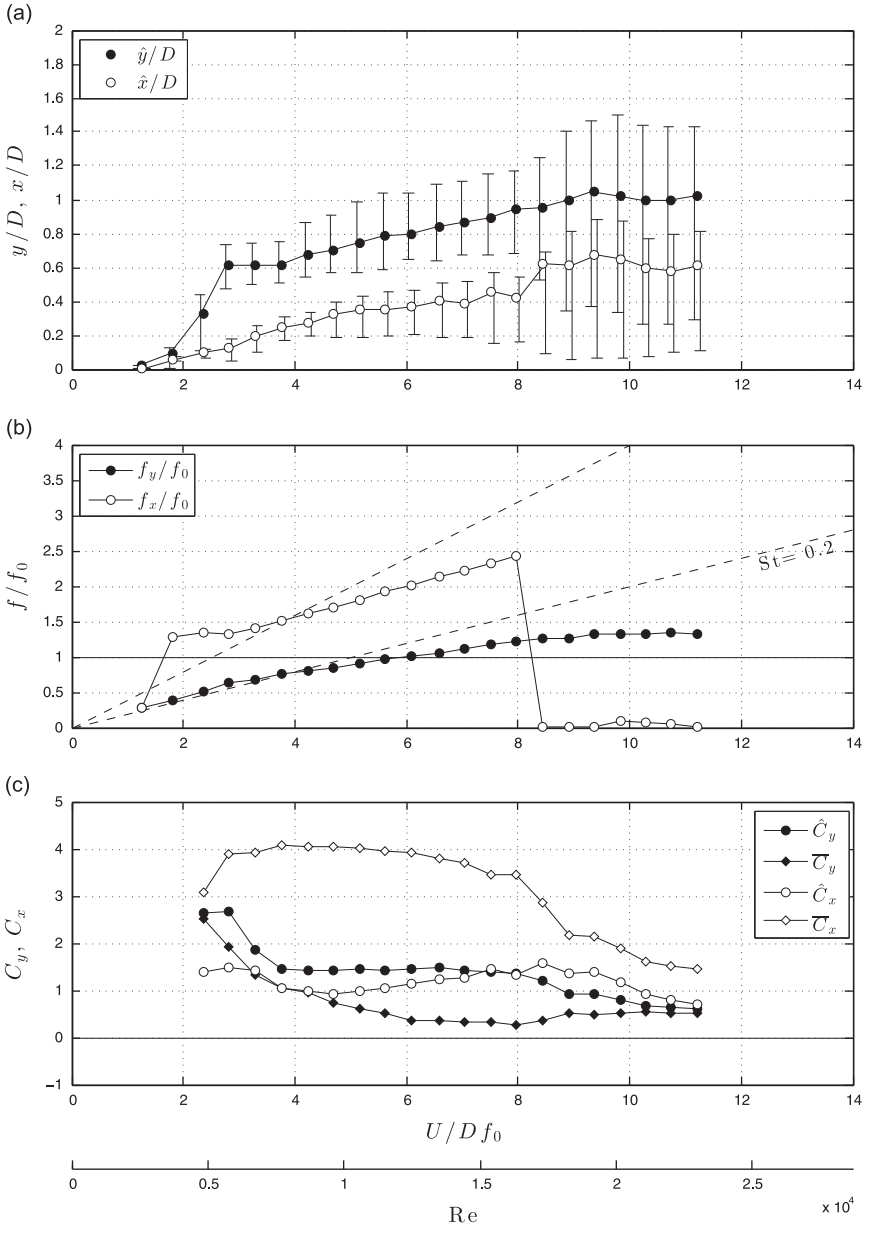

Fig. 14. WIV dynamic response of the downstream cylinder in staggered arrangement, $x_0/D = 4.0$ and $y_0/D = 2.0$. (a) Displacement and (b) frequency of vibration and (c) force coefficients.

This quasi-steady approach does not take into account the vortex wake from upstream, but only the steady effect of lift and drag. Also, this mechanism would not excite systems with 1-dof, since it requires an orbit in x and y for a positive input of energy. Naudascher and Rockwell (1994) comment that wake flutter, like other coupled instabilities, occurs only if the natural frequencies in the x and y directions are reasonably close, which is not the case for this experiment. But perhaps for a reduced range of reduced velocities, the WIV mechanism is able to bring both oscillation frequencies close together, as seen in Fig. 12(b), and extract energy from the flow in such a manner. (Note: Wake flutter has been called 'wake galloping' by Zdravkovich, 1997 and Blevins, 1990, but we prefer to stick to the terminology 'wake flutter' since it requires response in 2-dof to be sustained.)

Elliptical vibrations can happen in different regions of the wake wherever the steady velocity profile is favourable. The amplitude of the oscillation is directly related to the intensity of the lift and drag gradient in the wake, hence oscillations are reduced for larger separations as the steady force profiles get attenuated. Bokaian and Geoola (1984) and Assi et al. (2010) correctly noted that the fluid–elastic instability reported in their work was not be mistaken by the wake-flutter mechanism described above, since their experiment presented only a single degree of freedom.

For $y_0/D = 1.0$ we cannot directly employ the same wake-stiffness concept as we did for the tandem case. Assi et al. (2013) showed that the 'wake spring' in the 'wake-stiffness' concept is only considered to be linear for around $\pm 1D$ away from the centreline. Nevertheless, a close look in the spectrum of drag in Fig. 13 reveals the existence of two branches in the C_x signature. Perhaps there is a similar 'wake stiffness' effect acting for oscillations around $y_0/D = 1.0$ as well, which we cannot determine in the present work.

Hydrodynamic coefficients in Fig. 12(c) show a very similar behaviour to the tandem case, except for a small variation in $\overline{C}_y$ due to the asymmetric characteristic of wake interference. The presence of a steady force pushing the cylinder towards the centreline of the upstream wake is also noticeable in a small lateral drift in the trajectories of Fig. 6(c).

As we move further out of the centreline to the staggered arrangement with $y_0/D = 2.0$ the interference effect of the wake starts to weaken. Fig. 14(a) shows that the maximum cross-flow displacement for the reduced velocity range is now

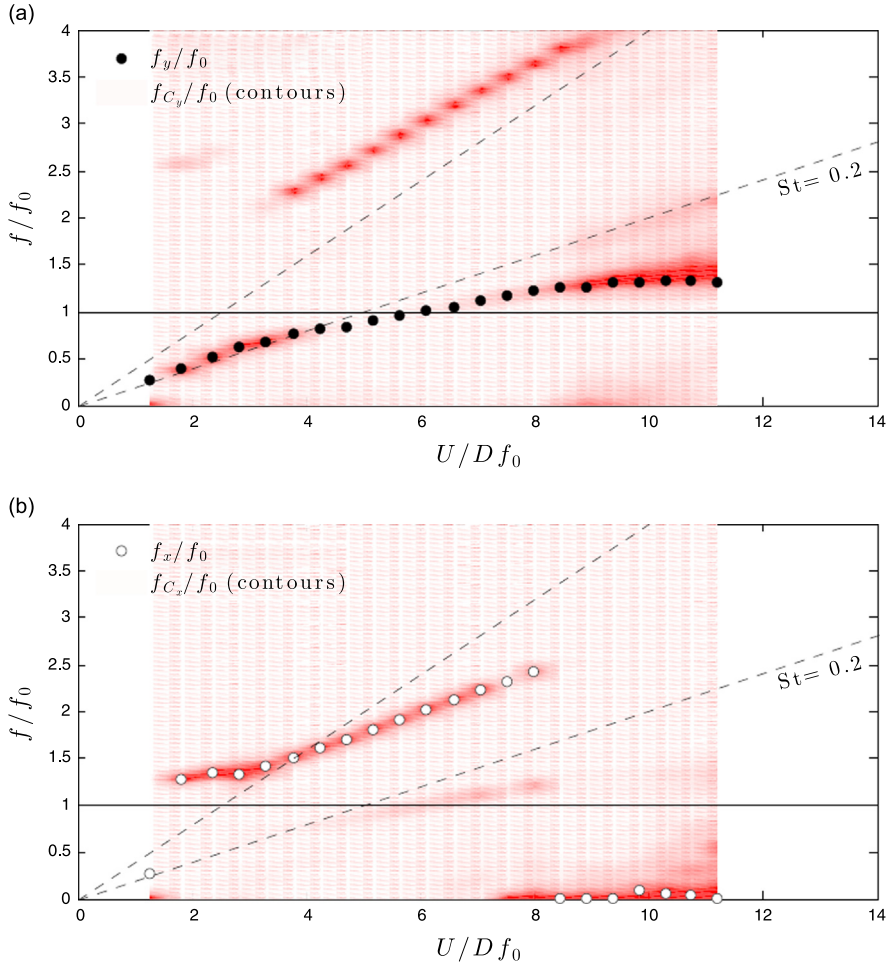

Fig. 15. Dominant frequency of vibration (symbols) and power spectrum (background red contours) of (a) lift and (b) drag for the downstream cylinder of a tandem pair: $x_0/D = 4.0$ and $y_0/D = 2.0$. (For interpretation of the references to colour in this figure caption, the reader is referred to the web version of this paper.)

reduced to $\hat{y}/D \approx 1.0$, even though $\hat{x}/D$ still shows the same levels as the previous separation. Vertical bars now decrease revealing a more well behaved envelope of vibration.

Fig. 14(b) shows that f_y/f_0 still follows a well behaved trend, also identified as the lowest branch in the C_y spectrum of Fig. 15(a). However, f_x/f_0 only shows a dominant frequency during the reduced velocity range in which resonant VIV is effective. After the end of the synchronisation region, for $U/Df_0 > 8$, no clear dominant frequency is identified in the streamwise motion, only slow drift and random vibrations as observed in Fig. 6; nevertheless they do amount to a significant amplitude of displacement. Also, no clear inferior branch is found in the C_x spectrum in Fig. 15(b), especially none related to the 'wake stiffness' concept.

Fig. 14(c) shows that $\overline{C}_x$ has increased as the cylinder moved out of the protected, low-speed region of the wake. But the most interesting result lies in the variation of $\overline{C}_y$ versus reduced velocity. One can imagine that as the cylinder oscillates with higher amplitudes it enters the region with stronger interference of the upstream wake. A lateral force will develop to

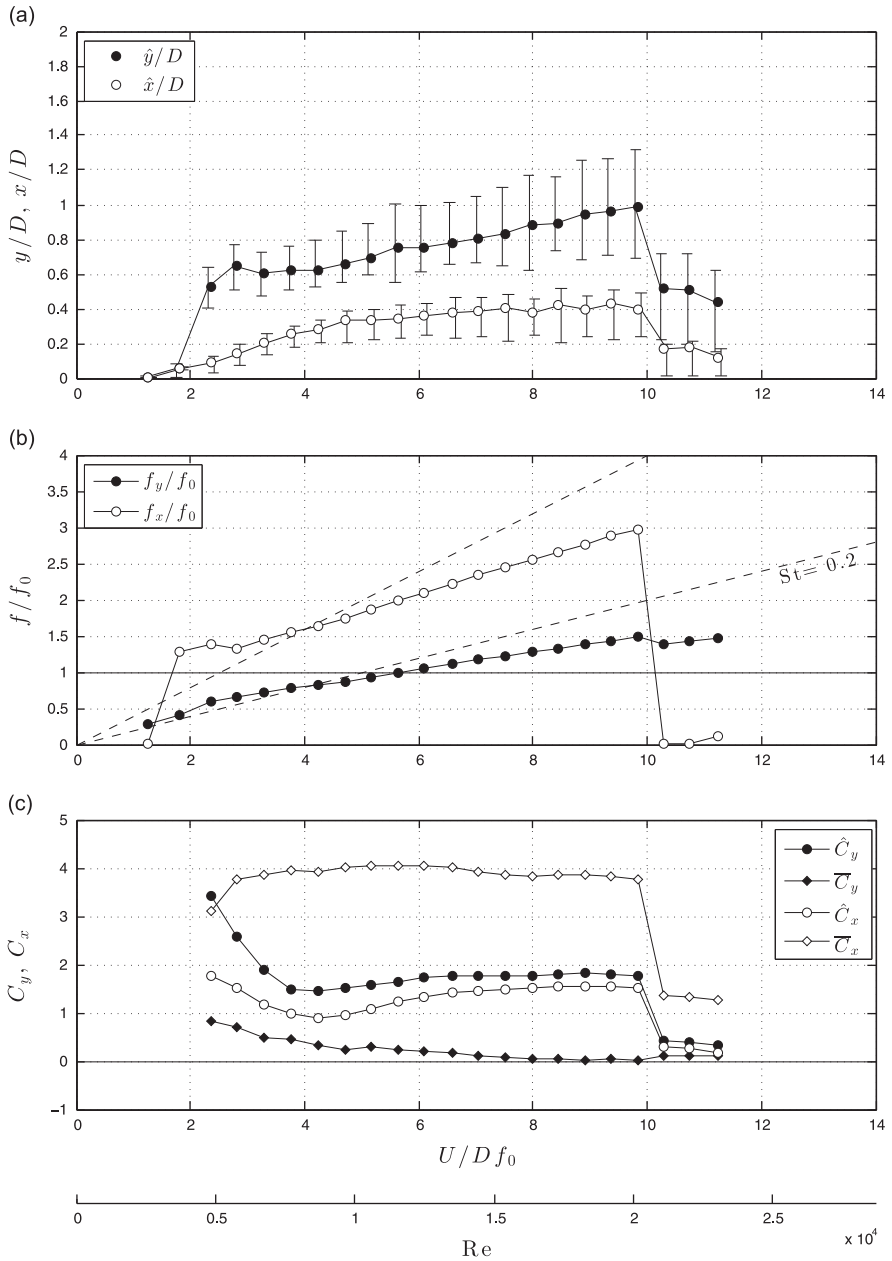

Fig. 16. WIV dynamic response of the downstream cylinder in staggered arrangement, $x_0/D = 4.0$ and $y_0/D = 3.0$. (a) Displacement and (b) frequency of vibration and (c) force coefficients.

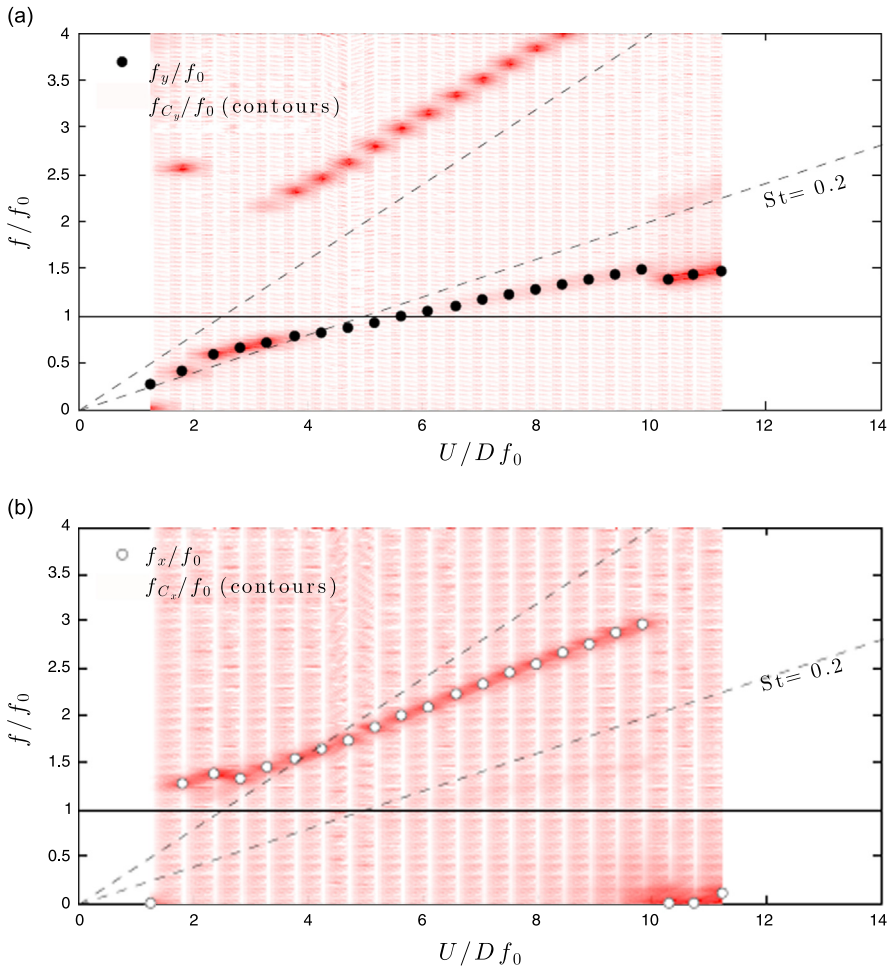

Fig. 17. Dominant frequency of vibration (symbols) and power spectrum (background red contours) of (a) lift and (b) drag for the downstream cylinder of a tandem pair: $x_0/D = 4.0$ and $y_0/D = 3.0$. (For interpretation of the references to colour in this figure caption, the reader is referred to the web version of this paper.)

draw the cylinder towards the centreline, thus changing the mean lift $\overline{C}_y$. However, this phenomenon turned out to be stronger for $y_0/D = 2.0$ and not the smaller separation.

Finally, Fig. 16 presents the results for the furthest staggered case of $y_0/D = 3.0$. We will limit to comment that at this lateral separation the downstream cylinder is too far out of the centreline to encounter significant interference from the upstream wake. Displacements, frequencies and forces all come back to be similar to the isolated cylinder case in VIV. Also, no signs of wake interference are noticeable in the spectrum of C_y and C_x in Fig. 17 either. With the exception of a small variation in $\overline{C}_y$, that should appear as the cylinder gets closer to the 'wake interference' region during vibration, the response seems to be driven by VIV and not WIV any longer.

5. Conclusion

In the present work we observed that the downstream cylinder of a pair is able to undergo 2-dof WIV for lateral separations between $y_0/D/0.0$ and 2.0. For a larger separation of $y_0/D = 3.0$ the cylinder was found to respond in a typical VIV behaviour.

For reduced velocities in the range between 1.5 and 12, the response was found to pass through a synchronisation range in which VIV is important. If reduced velocity is increased beyond this range, the WIV mechanism will dominate the 2-dof response in pretty much the same way it dominates 1-dof vibrations.

The WIV response in 2-dof is not qualitatively different from that observed for 1-dof systems oscillating in the cross-flow direction. Of course the branches of response take a different shape, but apart from that the general behaviour is monotonically increasing amplitude of displacement for increasing reduced velocity (or Reynolds number) was observed once more. The typical wake-flutter response, showing elliptical orbits, was not observed during the experiments, maybe

due to the frequency ratio being different from 1. For some specific flow speeds for $y_0/D = 1.0$ we might consider that wake-flutter was acting together with WIV

We have found evidence for a mechanism of 'wake stiffness' to be occurring for the 2-dof tandem arrangement and traces of it for $y_0/D = 1.0$. Further investigation is required to understand how the 'wake-stiffness' concept in 2-dof would differ from the 1-dof case.

Postscript: At the time of this paper going to print, Chaplin and Batten (2014) published a very interesting work concerning WIV of two cylinders with four degrees of freedom, two in each direction of motion. This is probably the work most similar to the present investigation and deserve the attention of the reader interested in WIV.

Acknowledgements

We are thankful to the kind contribution of Prof. Peter W. Bearman and the support from Imperial College (Dept. of Aeronautics) and CAPES Brazilian Ministry of Education (2668-04-1) at the time of the experiments. The author also acknowledges support from FAPESP (2013/07335-8) and CNPq (308916/2012-3) that allowed him time to revisit the data and write this manuscript.

References

Assi, G.R.S., 2009. Mechanisms for Flow-Induced Vibration of Interfering Bluff Bodies (Ph.D. thesis). Imperial College London, London, UK. Available from ⟨www.ndf.poli.usp.br/~gassi⟩.

Assi, G.R.S., Bearman, P.W., Carmo, B., Meneghini, J., Sherwin, S., Willden, R., 2013. The role of wake stiffness on the wake-induced vibration of the downstream cylinder of a tandem pair. Journal of Fluid Mechanics 718, 210–245.

Assi, G.R.S., Bearman, P.W., Kitney, N., 2009. Low drag solutions for suppressing vortex-induced vibration of circular cylinders. Journal of Fluids Structures 25, 666–675.

Assi, G.R.S., Bearman, P.W., Meneghini, J., 2010. On the wake-induced vibration of tandem circular cylinders: the vortex interaction excitation mechanism. Journal of Fluid Mechanics 661, 365–401.

Bearman, P.W., 1984. Vortex shedding from oscillating bluff bodies. Annual Review of Fluid Mechanics 16, 195–222.

Blevins, R., 1990. Flow-Induced Vibration, 2nd edition. Van Nostrand Reinhold, New York.

Bokaian, A., Geoola, F., 1984. Wake-induced galloping of two interfering circular cylinders. Journal of Fluid Mechanics 146, 383–415.

Chaplin, J.R., Batten, W.M.J., 2014. Simultaneous wake- and vortex-induced vibrations of a cylinder with two degrees of freedom in each direction. Journal of Offshore Mechanics and Arctic Engineering 136. Page numbers TBA.

Dahl, J., Hover, F., Triantafyllou, M., 2006. Two-degree-of-freedom vortex-induced vibrations using a force assisted apparatus. Journal of Fluids Structures 22, 807–818.

Jauvtis, N., Williamson, C.H.K., 2004. The effect of two degrees of freedom on vortex-induced vibration at low mass and damping. Journal of Fluid Mechanics 509, 23–62.

Naudascher, E., Rockwell, D., 1994. Flow-Induced Vibrations. An Engineering Guide, 1st edition. A.A. Balkema, Rotterdam.

Paidoussis, M., Price, S., deLangre, E., 2011. Fluid–Structure Interactions: Cross-Flow-Induced Instabilities, 1st edition. Cambridge University Press, New York.

Price, S., 1995. A review of theoretical models for fluid–elastic instability of cylinder arrays in crossflow. Journal of Fluids Structures 9, 463–518.

Price, S.J., 1975. Wake induced flutter of power transmission conductors. Journal of Sound Vibration 38, 125–147.

Price, S.J., Abdallah, R., 1990. On the efficacy of mechanical damping and frequency detuning in alleviating wake-induced flutter of overhead power conductors. Journal of Fluids Structures 4, 1–34.

Ruscheweyh, H.P., 1983. Aeroelastic interference effects between slender structures. Journal of Wind Engineering and Industrial Aerodynamics 14, 129–140.

Ruscheweyh, H.P., Dielen, B., 1992. Interference galloping-investigations concerning the phase lag of the flow switching. Journal of Wind Engineering and Industrial Aerodynamics 43, 2047–2056.

Simpson, A., 1977. In-line flutter of tandem cylinders. Journal of Sound Vibration 54, 379–387.

Simpson, A., Flower, J.W., 1977. An improved mathematical model for the aerodynamic forces on tandem cylinders in motion with aeroelastic applications. Journal of Sound Vibration 51, 183–217.

Sumner, D., 2010. Two circular cylinders in cross-flow: a review. Journal of Fluids Structures 26, 849–899.

Sumner, D., Price, S., Paidoussis, M., 2000. Flow-pattern identification for two staggered circular cylinders in cross-flow. Journal of Fluid Mechanics 411, 263–303.

Tsui, Y.T., Tsui, C.C., 1980. Two dimensional stability analysis of two coupled conductors with one in the wake of the other. Journal of Sound Vibration 69, 361–394.

Williamson, C.H.K., Govardhan, R., 2004. Vortex-induced vibrations. Annual Review of Fluid Mechanics 36, 413–455.

Zdravkovich, M.M., 1988. Review of interference-induced oscillations in flow past two circular cylinders in various arrangements. Journal of Wind Engineering and Industrial Aerodynamics 28, 183–200.

Zdravkovich, M.M., 1997. Flow Around Circular Cylinders, vol. 1, 1st edition. Oxford University Press, Oxford.

Zdravkovich, M.M., 2003. Flow Around Circular Cylinders, vol. 2, 1st edition. Oxford University Press, Oxford.